Discussion

In Table 1 the row $C_{M,1/4} = -0.09$ corresponds to a light airplane with a NACA-4412 airfoil, while the bottom row $C_{M,1/4} = -0.18$, represents the same airplane with a typical Wortman airfoil. Similar calculations show that at the same airspeed the use of the Wortman airfoil would nearly double the tail download. Equation (8) predicts $L_t = 0$ for $h = 0.454$ with the NACA-4412 airfoil. However, Eqs. (13) and (14) show that this is unstable since $h_{np} = 0.3264$, for $q_t/q = 1$.

References

[1]Naylor, C. H., "Notes on the Induced Drag of Wing-Tail Combination," British R&M 2528. July 1946.

[2]Laitone, E. V., "Positive Tail Loads for Minimum Induced Drag of Subsonic Aircraft," Journal of Aircraft, Vol. 15, No. 12, 1978, pp. 837–842.

[3]Durand, W. F., Aerodynamic Theory, Vol. 4, Springer-Verlag, Berlin, 1934, pp. 85, 86.

[4]Munk, M. M., Fundamentals of Fluid Dynamics for Aircraft Designers, Ronald Press, New York, 1929, pp. 76–83.

[5]Liu, H.-T., "Unsteady Aerodynamics of a Wortman Wing at Low Reynolds Numbers," Journal of Aircraft, Vol. 29, No. 4, 1992, pp. 532–539.

[6]McGhee, R. V., and Beasley, W. D., "Low-Speed Aerodynamic Characteristics of a 17-Percent Thick Airfoil Section Designed for General Aviation Applications," NASA TN D-7428, Dec. 1973.

[7]Perkins, C. D., and Hage, R. E., Airplane Performance Stability and Control, Wiley, New York, 1949, pp. 218, 229, 250.

[8]Laitone, E. V., "Lift Curve Slope for Finite-Aspect-Ratio Wings," Journal of Aircraft, Vol. 26, No. 8, 1989, pp. 789, 790.

Pressure Measurements on a Forward-Swept Wing-Canard Configuration

Giovanni Lombardi*
University of Pisa, Pisa 56126, Italy
and
Mauro Morelli†
CSIR Laboratory, Pretoria 0001, South Africa

Nomenclature

b = wing span, m
C_l = lift coefficient of the wing
$C_{l\alpha}$ = slope of the wing lift coefficient at low incidence
$C_{l,max}$ = maximum lift coefficient of the wing
C_l = wing sectional lift coefficient
$C_{l\alpha}$ = slope of the wing sectional lift coefficient at low incidence
c = chord length, m
c_p = pressure coefficient
L = stagger, horizontal distance between the points at $x/c = 0.3$ of the chords of the wing and the canard, at the root section, m
M = Mach number
T = gap, vertical distance between the points at $x/c = 0.3$ of the chords of the wing and the canard, at the root section, m

x = distance measured from wing section leading edge, m
y = distance along the span measured from wing root, m
α = angle of attack
α_u = angle of attack of maximum lift
γ = decalage, angle defined by the directions of the wing and canard chords, Fig. 1
Δc_p = pressure coefficient jump across the shock wave
η = $y/(b/2)$
Λ = angle of sweep at $\frac{1}{4}$ of the chord

Introduction

IN Ref. 1, the effects of a fore sweep, in the subsonic and transonic regimes, are studied; one of the main features arising from that analysis is that, as could be expected, the flow on a forward-swept wing separates first in the root region. This suggests the inclusion of some aerodynamic devices producing a favorable interference effect in that region (e.g., a lifting canard or a strake), in order to obtain a more uniform stall condition along the span. This could give a further advantage in the use of a forward-swept wing, which provides, in any case, the potential for increasing aerodynamic efficiency.[2]

For low angles of attack and low subsonic flows, the study of the canard-wing configurations, with fairly accurate results, can be performed by means of nonlinear potential numerical methods,[3-6] but, for high Mach numbers or high angles of attack, experiments are necessary, at least at the present state of the computational capabilities.

Experimental Setup

Pressure measurements on 320 points of the wing surface, as detailed described in Refs. 1 and 7, were carried out in the Medium Speed Wind Tunnel of the CSIR Laboratories, in South Africa. This is a closed circuit pressurized tunnel, with a confined square test section, 1.5 m in width and 4.5 m in length, enclosed in a plenum.

The adopted geometric conventions are shown in Fig. 1; taking also into account the tests carried out in Ref. 8, the relative position between wing and canards was chosen to be characterized by a fixed stagger of 2.26 wing mean geometric chords, and vertical positions with gaps T/L (Fig. 1) of -0.166, 0, and 0.166 (low, medium, and high positions). In the present Note no cases with decalage angles are considered.

One of the wing models already tested in Ref. 1 was used; it is a wing with zero twist and dihedral angles, aspect ratio 5.7, taper ratio 0.4, sweep angle $\Lambda = -25$ deg at $\frac{1}{4}$ of the chord, and a NACA 0012 wing section. The canard model was a unswept rectangular lifting surface with zero twist and dihedral angles, aspect ratio 4, NACA 0012 wing section, and a span of 0.47 times the wing span.

Due to the basic nature of the research, special attention was paid to the effects produced on the wing by the canard, and therefore the measurements were performed only on the wing at Mach numbers of 0.3 and 0.7, with a Reynolds number $\approx 2.8 \times 10^6$. Test conditions, model characteristics, and pressure orifice (0.5-mm diam) location are described in Ref. 1.
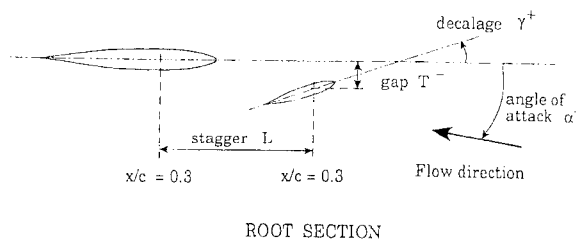
*Assistant Professor, Department of Aerospace Engineering, Diotisalvi, 2.
†Research Engineer, Medium Speed Wind Tunnel, P.O. Box 395.

Fig. 1 Geometric conventions.

C_l along the span (nondimensionalized with the dynamic pressure and the local wing chord) and the global C_L (nondimensionalized with the dynamic pressure and wing planform surface) were evaluated by means of numerical integration of the pressure distributions.

Results and Discussion

Low Angles of Attack

The considered configurations, with corresponding $C_{L\alpha}$ (evaluated by means of the measurements at $\alpha = 0$ and $\alpha = 4$ deg), are reported in Table 1.

At $M = 0.3$, a general reduction of the wing lift curve slope is evident, depending on the downwash in the inner portion of the wing, greater than the upwash in the outer zone (Fig. 2). Thus, the effect of the canard is to move the load toward the tip, with an increase in the outer zone and a reduction in the inner one. Stronger effects are present when the canard is in low or coplanar position, because of the stronger interference between the wing and the wake of the canard.

At $M = 0.7$, shock waves on the wing are present even at low angles of attack,[1] and this substantially modifies the effects of interference.

By analyzing Table 1 and Fig. 3, the behavior is found to be as in the subsonic regime, although with quite different quantitative effects; a stronger effect can be observed when the canard is in a coplanar position. This is related to the strong interference between the wake of the canard and the shock wave on the wing. The canard produces a downwash exactly in the zone in which the shock wave is present on the

isolated forward swept wing,[1] giving a strong reduction in its intensity (see e.g., Fig. 4): the shock wave, present at the root of the isolated wing with a $\Delta c_p \approx 0.5$, practically disappears. Attention must be paid to choosing the canard position; it is also possible to increase the shock wave intensity. When the wake passes very close to the upper wing surface, it produces a considerable velocity increase in the zone of the wing crossed by the canard tip vortex, resulting in a stronger shock wave. This happens, e.g., at an angle of attack of 4 deg in the configuration with coplanar canard: a strong shock wave, $\Delta c_p \approx 0.7$, is present around $\eta \approx 0.5$ (Fig. 5).

High Angles of Attack

The canard-wing interference effects at high angles of attack are strongly dependent on the canard position. For $M = 0.3$, a clear-cut tendency of the $C_{L\max}$ to lower values is present (Table 2); on the contrary, the $C_{L\max}$ values increase at $M = 0.7$, with corresponding angles of attack that are much higher than for the isolated wing.

At $M = 0.3$, with the canard in high position, the stall is similar to that of the isolated wing. Conversely, the stall behavior is substantially different for medium or low position. By analyzing Fig. 6 it is evident that with the canard in a low

Table 1 Wing lift curve slope at low angles of attack

	Isolated wing	With high canard	With medium canard	With low canard
$M = 0.3$	0.0730	0.0657	0.0624	0.0597
$M = 0.7$	0.0785	0.0699	0.0684	0.0682

Table 2 Wing maximum lift conditions

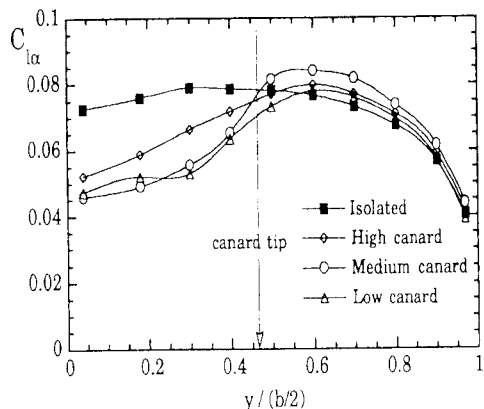|	Isolated wing	With high canard	With medium canard	With low canard
$M = 0.3$				
$C_{L\max}$	1.173	1.142	1.061	0.944
α_{st}	19.8	19.7	18.2	22.2
$M = 0.7$				
$C_{L\max}$	0.677	0.768	0.758	0.776
α_{st}	11.3	17.4	17.4	21.8

Fig. 2 Sectional lift slope coefficients along the wing span, $M = 0.3$.

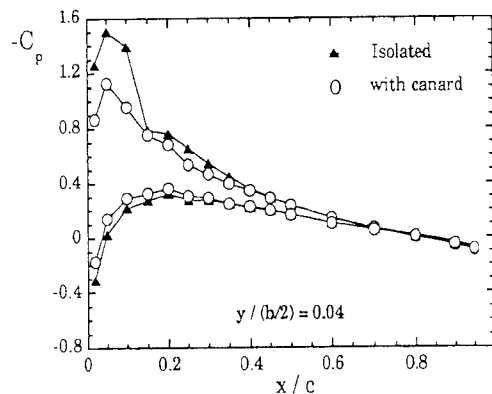Fig. 3 Sectional lift slope coefficients along the wing span, $M = 0.7$.

Fig. 4 Pressure distributions in chord; $M = 0.7$, low canard-$\alpha = 4$ deg.
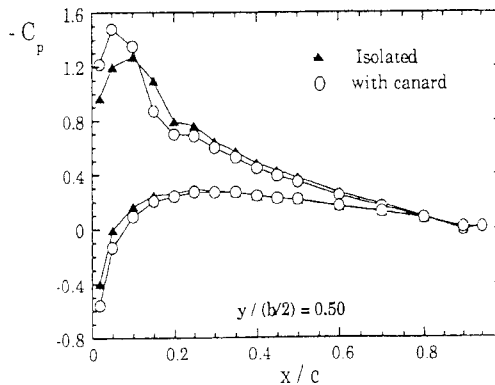

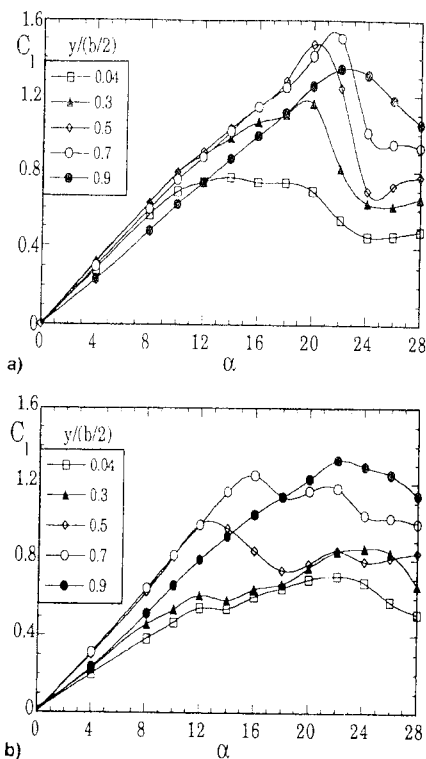Fig. 5 Pressure distributions in chord; $M = 0.7$, medium canard-$\alpha = 4$ deg.

Fig. 6 C_l-α cures for several wing span stations, $M = 0.3$: a) isolated wing and b) low canard.
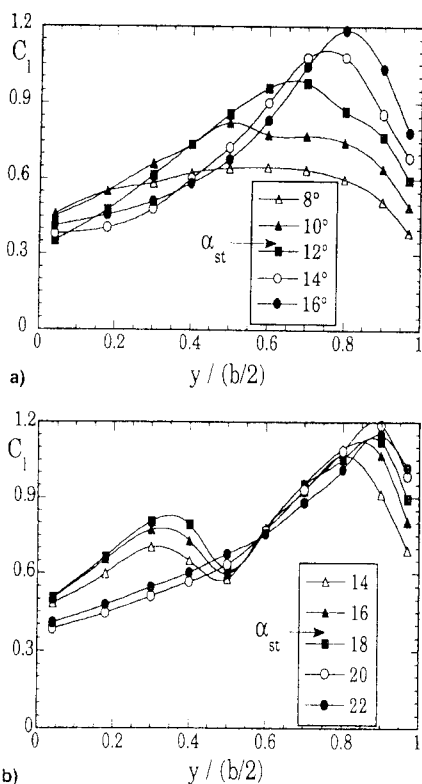

Fig. 7 Wing spanwise C_l curves near stall and poststall. $M = 0.7$: a) isolated wing and b) medium canard.

position. the sections near the wing root reach the stall conditions at higher angles of attack (≈ 22 deg vs 16 deg for the isolated wing). but with lower values of the lift coefficient. whereas in the outer zone the stall is anticipated by the canard. with a lower α_{st} (from 14 deg at $\eta = 0.6$ to 20 deg for $\eta = 0.9$) and far lower values of the lift coefficient. We can also note that with this canard configuration, there is a "soft" stall behavior. characterized by the absence of the marked dis-
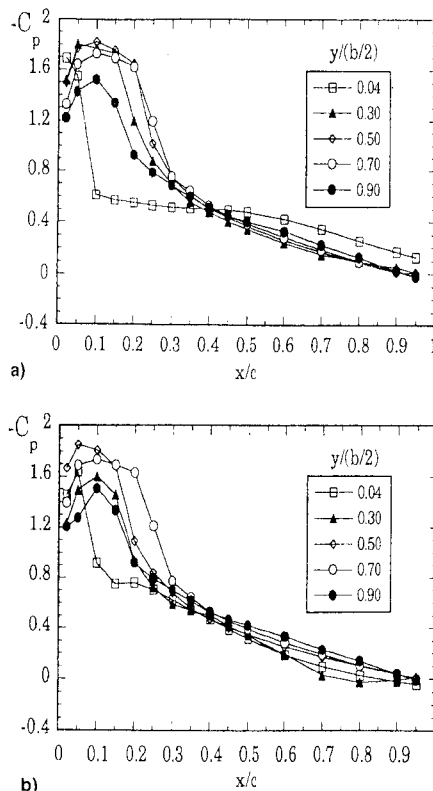

Fig. 8 Pressure distributions in chord (upper surface), $M = 0.7$-$\alpha = 8$ deg: a) isolated wing and b) low canard B.

placement of the pressure center towards the tip, typical of the isolated wing.

At $M = 0.7$, in the configurations with canard, the wing stall occurs at much higher angles of attack (Table 2), with values of $C_{l.max}$ greater than for the isolated wing. From Fig. 7 it is clear that the stall behavior along the span is quite different. Under stall conditions the wing in interference with the canard presents a greater load at the root (up to $\eta \approx 0.4$), with respect to the isolated one, and approximately the same load in the outer zone. This very significant difference can be explained by analyzing the pressure distribution along the chord. In Fig. 8a, a well-defined shock wave can be observed at the root of the isolated wing ($\Delta c_p \approx 1$), and a smaller, almost constant one is present along the whole span ($\Delta c_p \approx 0.85$ from $\eta \approx 0.15$ to $\eta \approx 0.85$). In the configuration with the low canard (Fig. 8b), the shock wave at the root is of a lower intensity ($\Delta c_p \approx 0.75$); as a consequence, there is a clearly less extended boundary-layer separation.

Conclusions

The shown results provided some information on basic canard-wing flow, both in the subsonic and in transonic regimes.

The canard effects are significantly dependent on canard position. In particular, by utilizing a high positioned canard, very small variations in the aerodynamic characteristics of the wing can be obtained. Conversely, low or coplanar canard positions greatly affect the aerodynamic behavior of the wing.

From the aerodynamic viewpoint, the lift distribution on a forward-swept wing, particularly at high angles of attack, can be turned to a real advantage when coupled with a canard control surface; under these conditions the canard wake induces a downwash at the wing root as well as an upwash at the wing tip, so that more uniform stall conditions along the span are obtained. More specifically, in the case of transonic flow, coupling a canard control surface with a forward-swept wing appears to be a very efficient configuration, because the flow induced by the canard can reduce the strong shock wave present at the root of the isolated wing. It is also important to note that with a suitable choice of the canard geometry

and position, in the transonic regime an increase in C_{L_α} is even possible.

References

[1]Lombardi, G., "Experimental study on the Aerodynamic Effects of a Forward Sweep Angle," *Journal of Aircraft* (to be published).

[2]Spact, G., "The Forward Swept Wing: A Unique Design Challenge," AIAA Paper 80-1885, Aug. 1980.

[3]Mann, M. J., "A Forward-Swept-Wing Fighter Configuration Designed by a Transonic Computational Method," *Journal of Aircraft*, Vol. 23, No. 6, 1986, pp. 506–512.

[4]Feistal, T. W., Corsiglia, V. R., and Levin, D. B., "Wind Tunnel Measurements of Wing-Canard Interference and a Comparison with Various Theories," Society of Automotive Engineers TP 810575, 1981.

[5]Behr, R. J., and Wagner, S. N., "Application of a Low Order Panel Method to Slender Delta-Wings at High Angles of Attack," *Boundary Integral Methods. Theory and Applications*, Springer-Verlag, Berlin, 1991, pp. 105–114.

[6]Buresti, G., Lombardi, G., and Petagna, P., "Wing Pressure Loads in Canard Configurations: A Comparison Between Numerical Results and Experimental Data," *The Aeronautical Journal*, Vol. 96, Aug./Sept. 1992, pp. 271–279.

[7]Buresti, G., Lombardi, G., and Morelli, M., "Pressure Measurements on Different Canard-Wing Configurations in Subsonic Compressible Flow," Atti del Dipartimento di Ingegneria Aerospaziale, Univ. of Pisa, ADIA 91-4, Sept. 1991.

[8]Buresti, G., and Lombardi, G., "Indagine Sperimentale Sull'Interferenza Ala-Canard," *L'Aerotecnica, Missili e Spazio*, Vol. 67, Nos. 1–4, 1988, pp. 47–57.